

**AFRL-SN-HS-TR- 2002-041**

---

**MULTISPECTRAL DETECTOR ARRAY TECHNOLOGY**

**Nan Marie Jokerst  
School of Electrical Engineering  
Microelectronics Research Center  
Georgia Institute of Technology  
Atlanta Georgia 30332-0250**

**FINAL REPORT: March 1998 – December 1999**

**APPROVED FOR PUBLIC RELEASE: DISTRIBUTION UNLIMITED**



**AIR FORCE RESEARCH LABORATORY  
Sensors Directorate  
80 Scott Dr  
Hanscom AFB MA 01731-2909**

---

**20021202 066**

## TECHNICAL REPORT

**Title: Multispectral Detector Array Technology**

## PUBLICATION REVIEW

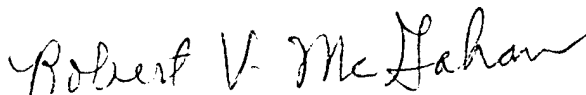
**This report has been reviewed and is approved for publication:**

**APPROVED:**



**CHARLES WOODS**  
AFRL/SNHC  
Optoelectronic Technology Branch  
Electromagnetics Technology Division

**APPROVED:**



**ROBERT V. MCGAHAN**  
Technical Advisor  
Electromagnetics Technology Division

| REPORT DOCUMENTATION PAGE   |   |   | Form Approved<br>OMB No. 0704-0188 |  |
|---|---|---|------------------------------------|--|
| Public reporting burden for this collection of information is estimated to average 1 hour per response, including the time for reviewing instructions, searching existing data sources, gathering and maintaining the data needed, and completing and reviewing the collection of information. Send comments regarding this burden estimate or any other aspect of this collection of information, including suggestions for reducing this burden, to Washington Headquarters Services, Directorate for Information Operations and Reports, 1215 Jefferson Davis Highway, Suite 1204, Arlington, VA 22202-4302, and to the Office of Management and Budget, Paperwork Reduction Project (0704-0188), Washington, DC 20503.  |   |   |                                    |  |
| 1. AGENCY USE ONLY (Leave blank)  | 2. REPORT DATE<br>13 December 1999                          | 3. REPORT TYPE AND DATES COVERED<br>Final -- 12 March 1998 - 14 December 1999                             |                                    |  |
| 4. TITLE AND SUBTITLE<br>Multispectral Detector Array Technology  |   | 5. FUNDING NUMBERS<br>C: F30602-98-1-0115<br>PE: 61102F<br>PR: E-8-7272<br>PROJ: 2305<br>TA: FR<br>WU: P1 |                                    |  |
| 6. AUTHOR(S)<br>Nan Marie Jokerst   |   | 8. PERFORMING ORGANIZATION<br>REPORT NUMBER   |                                    |  |
| 7. PERFORMING ORGANIZATION NAME(S) AND ADDRESS(ES)<br>School of Electrical Engineering<br>Microelectronics Research Center<br>Georgia Institute of technology<br>Atlanta, GA 30332-0250   |   | 10. SPONSORING/MONITORING<br>AGENCY REPORT NUMBER<br><br>AFRL-SN-HS-2002-041                              |                                    |  |
| 9. SPONSORING/MONITORING AGENCY NAME(S) AND ADDRESS(ES)<br>Philip R. Hemmer<br>Air Force Research Laboratory/SNHC<br>80 Scott Drive<br>Hanscom AFB, MA 01731-2909   |   |   |                                    |  |
| 11. SUPPLEMENTARY NOTES   |   |   |                                    |  |
| 12a. DISTRIBUTION AVAILABILITY STATEMENT<br>Approval for public release; distribution unlimited   |   | 12b. DISTRIBUTION CODE<br><br>a   |                                    |  |
| 13. ABSTRACT (Maximum 200 words)<br>A sensor is a device used to sense or measure physical phenomena. Thus, sensors may detect electrical, mechanical, optical, chemical, tactile, or acoustic signatures of an object or scene. Objects that may be difficult to discriminate using a single sensor are often differentiated with a multiple sensor system that exploits several signature phenomena. The application of multiple sensors (and the fusion of their data) offers numerous potential performance benefits over traditional single sensor approaches. In our application, which is infrared target discrimination, employing multiple sensors, which respond to different signatures, increases the probability that a target signature will be found against a given set of weather, clutter or background noise sources. A multiple sensor system, in other words, diminishes ambiguity and uncertainty in the measured information by reducing the set of hypotheses about the target or event. Multiple sensors may also be used to reduce the vulnerability to false conclusions drawn from data of a single sensor. For instance, missiles may carry multiple sensors to better guarantee a hit or a radar can use multiple sensors to counter-jam incoming missiles. |   |   |                                    |  |
| 14. SUBJECT TERMS<br>Sensors  |   | 15. NUMBER OF PAGES<br>16   |                                    |  |
|   |   | 16. PRICE CODE  |                                    |  |
| 17. SECURITY CLASSIFICATION<br>OF REPORT<br>UNCLASSIFIED  | 18. SECURITY CLASSIFICATION<br>OF THIS PAGE<br>UNCLASSIFIED | 19. SECURITY CLASSIFICATION<br>OF ABSTRACT<br>UNCLASSIFIED  | 20. LIMITATION OF ABSTRACT<br>UL   |  |

## Table of Contents

|      |                               |   |
|------|-------------------------------|---|
| I.   | Introduction.....             | 1 |
| II.  | Goal of the Research.....     | 5 |
| III. | Fabrication.....              | 6 |
| IV.  | Progress in the Research..... | 7 |

## List of Figures

|   |    |
|---|----|
| Figure 1 Schematic single-pixel architecture of the multispectral polarimetric sensor .....   | 5  |
| Figure 2 Processing flowchart for the triple-decker spectral Polarizer plate.....             | 6  |
| Figure 3 Calculated optimum structure of the multilayer subfilters .....                      | 7  |
| Figure 4 Optimum structure of the multispectral filters calculated for sapphire substrates... | 8  |
| Figure 5 Calculated sensitivity of the multispectral filter to the thickness variation.....   | 9  |
| Figure 6 Transmission characteristic of multispectral filter on GaAs substrate design.....    | 10 |
| Figure 7 Transmission of the multispectral filter on sapphire.....                            | 11 |
| Figure 8 Schematics of the model in the wire-grid polarizer simulation.....                   | 12 |
| Figure 9 Effect of grating height (A1 grating on sapphire substrate).....                     | 13 |
| Figure 10 Effect of pitch at grating height = 0.75mm (A1 grating on sapphire substrate).....  | 13 |
| Figure 11 Transmittance of quartz mask for wire-grid polarizer.....                           | 14 |

# Multispectral Sensing Technology

## I. Introduction

A sensor is a device used to sense or measure physical phenomena. Thus, sensors may detect electrical, mechanical, optical, chemical, tactile, or acoustic signatures of an object or scene. Objects that may be difficult to discriminate using a single sensor are often differentiated with a multiple sensor system that exploits several signature phenomena. The application of multiple sensors (and the fusion of their data) offers numerous potential performance benefits over traditional single sensor approaches. In our application, which is infrared target discrimination, employing multiple sensors, which respond to different signatures, increases the probability that a target signature will be found against a given set of weather, clutter, or background noise sources. A multiple sensor system, in other words, diminishes ambiguity and uncertainty in the measured information by reducing the set of hypotheses about the target or event. Multiple sensors may also be used to reduce the vulnerability to false conclusions drawn from data of a single sensor. For instance, missiles may carry multiple sensors to better guarantee a hit or a radar can use multiple sensors to counter-jam incoming missiles.

The goal of the research herein is to develop an integrated sensor capable of discriminating (multi) spectral and polarization signatures of a target and to achieve improved image contrast from the measured information. Infrared multispectral signatures of man-made systems depend on the surface coating of the object and/or chemical composition of the materials used. Moreover, multispectral data are significantly less sensitive to viewing geometry and surface smoothness than polarization data. On the other hand, polarimetric measurements take advantage of the fact that natural backgrounds show generally little or weak polarization signatures (with the exception of water), while man-made targets tend to radiate with preferential polarization components.<sup>1</sup> A recent study for MWIR (3-5 $\mu$ m) demonstrates that the polarized signatures of many natural objects were measured to be less than 0.2%, compared to 2-4% degree-of-polarization for man-made ground targets.<sup>2,3</sup> In addition, polarization data often contain information about the surface orientation and/or surface properties of objects, and a polarization signal can exist even when no intensity contrast is present. Consequently, it is believed that polarization and multispectral imaging data are complementary. Better contrast can thus be achieved by combining both, since they depend on different optical characteristics of the target. However, it is not clear yet what combinations of polarization and spectral measurements are optimal for target discrimination in a given scenario, since little data has been taken in natural and man-made scenes.

There have been continuing efforts to build multispectral and/or polarimetric sensors for a variety of applications in astronomy and the Earth sciences. Rather recently, such sensor systems have been developed for remote sensing and military applications. Some of the previous approaches to multispectral and/or polarimetric sensors are reviewed in the following sections.

#### A. Multiple-polarization/multiple-band systems

##### (1) EOSP (Earth Observing Scanning Polarimeter)<sup>4,5,6,7</sup>

The EOSP is an instrument, developed for Earth Observing System (EOS) space mission platforms at NASA, to provide global mapping with multispectral photopolarimetry. This enables a more pronounced aerosol signature in the polarization of the scattered light, compared to the radiance. The EOSP scans a continuous sweep of the instantaneous field of view (IFOV) of the scene. The scanned scene is supplied to eight boresighted telescope and aft optics assemblies simultaneously, each of which angularly separates the incident scene flux into two orthogonally-polarized beams. Each beam is then spectrally separated into three spectral bands using dichroic beamsplitters and bandpass filters. The spectral band of the system thus covers 12 discrete passbands, ranging from 410 nm to 2250 nm.

##### (2) POLDER (POLarization and Directionality of Earth Reflectances)<sup>8</sup>

The POLDER is an optical imaging radiometer, developed at CNES (Centre National d'Etudes Spatiales), France, and was installed on a satellite of the Japanese ADEOS mission in 1995. It scans a wide field of view (50°) with moderate spatial resolution (6 km) and observes bidirectional reflectance and polarization distribution of the scanned scene on a global scale by taking, for a given target, measurements in variable viewing configurations along the track of the satellite. The radiation from the scene is time-multiplexed by the fast-spinning spectral filters in nine spectral bands of the visible – near infrared spectrum. Polarization states are measured at three of the nine wavelengths.

### (3) POLARIS II<sup>9</sup>

POLARIS II is an imaging spectropolarimeter for ground-based astronomy, based on acousto-optic tunable filter (AOTF) technology. It was constructed at NASA/GSFC (Goddard Space Flight Center). An AOTF is a crystal which diffracts an incoming light beam into different directions, dependent upon the wavelength and the polarization state of the light, when an acoustic wave propagates through the crystal. When the incoming beam leaves the AOTF, the diffracted beams become polarized with +1 and -1 orders polarized orthogonally. The system is limited by the AOTF, since the wavelength tuning range is fundamentally restricted by the crystal of the AOTF and it allows only two linear polarization components.

### (4) Fourier-Transform IR Spectropolarimeter (FTIRSP)<sup>10,11</sup>

The FTIRSP measures the infrared Mueller matrix spectrum in transmission or reflection at 45° from a sample under test. A Michelson interferometer provides a sample beam of selected wavelength out of the global IR source by fine-tuning the position of a mirror. The whole spectrum thus covers 2.5~14μm. The polarization generator, composed of an achromatic retarder and a wire-grid polarizer, then polarizes the incident monochromatic light along the desired polarization direction. After the beam is scattered by the sample, its polarization state is analyzed by the polarization analyzer. The Mueller matrix of the sample for a specific wavelength and incident angle (45°) can be determined from the data. Applications include testing of polarization elements such as electro-optic modulators, IR polarizers, and retarders and IR signature modeling of military target samples.

### (5) REMIDS (Remote Minefield Detection System)<sup>12</sup>

The REMIDS is a multi-channel active/passive sensor system, developed by U.S. Army and operated on U.S. Army UH-60A Black Hawk helicopter to detect landmines. The system has 6 separate channels which includes p- and s- polarized laser reflectance measurements at  $\lambda=1.064\mu\text{m}$  and thermal emission for  $\lambda=8-12\mu\text{m}$ .



## B. Multiple-polarization/single-band system

### (1) MWIR Polarization Sensitive Thermal Imager<sup>13</sup>

In this system, the radiation from the target, after being transmitted through a wire-grid polarizer array, is imaged on a thermal imaging focal plane array. The wire-grid polarizer has three angular orientations, patterned using microlithography. The system covers 3-5  $\mu\text{m}$  wavelengths.

### (2) Diffraction Grating Photopolarimeter<sup>14,15</sup>

A diffraction grating is used to make a division-of-amplitude photopolarimeter. The incident light beam is diffracted at a diffraction grating and photodetectors detect the diffracted orders of the light. Four Stokes parameters are then extracted from the measured data. The dispersion of the grating poses a significant limit on the performance of the system.

### (3) Airborne MWIR Polarimetric Imager<sup>16</sup>

The incoming scene flux is divided into two polarization components by a Ge Brewster plate. Each of the polarized scenes from both reflected and transmitted beams is imaged sequentially in time on the IR camera. The most critical issue of the system is the band-to-band channel misregistration, which arises due to the sequential nature of the system.

It may be interesting to note the fundamental limits of some systems. Those which are based on time multiplexing require careful consideration about the misregistration between channels taken at different times. Alternatively, some systems are limited by using certain optical elements. For example, an AOTF imposes a fundamental limitation on the usable wavelength and on the number of polarization orientations. On the other hand, diffraction gratings result in a higher level of dispersion in the system. Most of the systems described above do not operate in the MWIR range, and none integrate polarizers with spectral filters in a compact single package. This may be due to the difficulty associated with the fabrication of the polarizer, in contrast to the wide availability of the off-the-shelf discrete optical elements.

## II. Goal of the Research

This study explores the integrated nature of multiple sensor fusion by designing and building a smart pixel sensor. This sensor integrates optical components that can determine spectral content, polarization state, and intensity level in each pixel. It can then post-process the multiple outputs of each pixel with a neural network based sensor fusion processor to perform target discrimination. This approach may permit highly selective discrimination among objects or targets with nearly identical spatial and spectral features, along with the compactness, portability, ruggedness, and signal processing strengths achieved through the use of silicon or GaAs integrated circuit technology.

Figure 1 shows the schematic diagram of the two different structures for the sensor. The triple-decker system on the right has a multilayer interference filter and a wire-grid polarizer on top of each other, while the polarization and spatial filters are laid side-by-side in the system on the left. Compared to the left hand side system, the triple-decker has lower resolution and is less power-efficient. The triple-decker system, however, has the data from spectral and polarization subpixels perfectly registered, and moreover, it is much easier to process due to the planar structure, lending itself as the only practical alternative for this study.

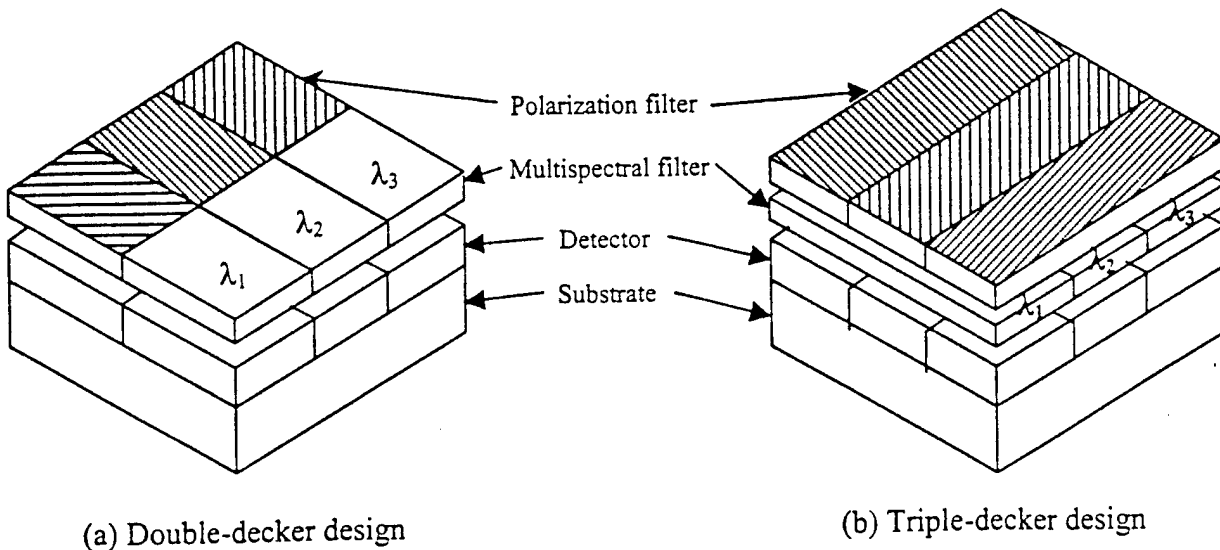


**Figure 1 Schematic single-pixel architecture of the multispectral polarimetric sensor**

### III. Fabrication

A discrete-component approach was used first to establish the operational feasibility of such a sensor concept in the 3–5  $\mu\text{m}$  waveband. More specifically, thin-film wire-grid polarizers and three spectral interference filters were vacuum deposited separately onto thin pixellated sapphire substrates, which were then mechanically contacted to form a multispectral-polarizer plate. The processing steps of the multispectral filter and the wire-grid polarizer are discussed in the next paragraph. This component will be evaluated by imaging calibrated laboratory targets such as rods, cones and cubes with a  $\text{CaF}_2$  infrared lens onto the spectral polarizer plate, and then reimaging the filtered image onto a commercially available Pt-Si camera.

Next, the fabrication of an integrated multispectral polarizer filter was attempted by depositing a wire-grid polarizer on spectral interference filter. Figure 2 represents the processing flowchart for the triple-decker system employing a 4-layer multispectral filter on the substrate. In Step 1, three layers of SiO/Ge/SiO are sputtered on the entire substrate (in the case of the three-layer-filter on sapphire, Step 1 is first two layers only (Ge/SiO)). Steps 2 and 3 involve optical lithography followed by selective dry etching of the upper SiO layer to define the three multispectral sub-pixels. Processing steps up to Step 3 are exactly the same as the multispectral plate. In Step 4, the final Ge layer is deposited on top of the three previous layers. In Step 5, fine metal wire ( $\sim 0.6\mu\text{m}$  wide) is then patterned (using optical lithography on thermally-evaporated Al) to form the polarization filters. Since the structure is not planarized, the polarization filter in Step 5 will likely have discontinuities. This structural discontinuity may not be a substantial

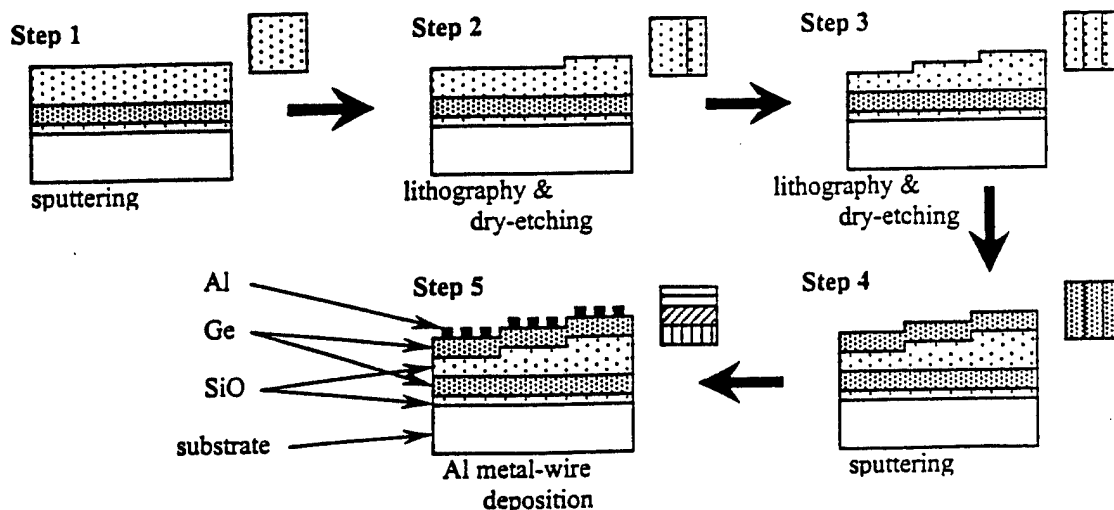


Figure 2. Processing flowchart for the triple-decker spectral Polarizer plate

problem, considering that the vertical step ( $\sim 0.25 \mu\text{m}$ ) is smaller than the pitch of wire grid ( $\sim 1.2 \mu\text{m}$ ). The integrated multispectral polarimetric sensor will be characterized similarly to the mechanically contacted sensor.

#### IV. Progress in the research

##### 1. Materials

Germanium (Ge) and silicon monoxide (SiO) were chosen as the interference filter

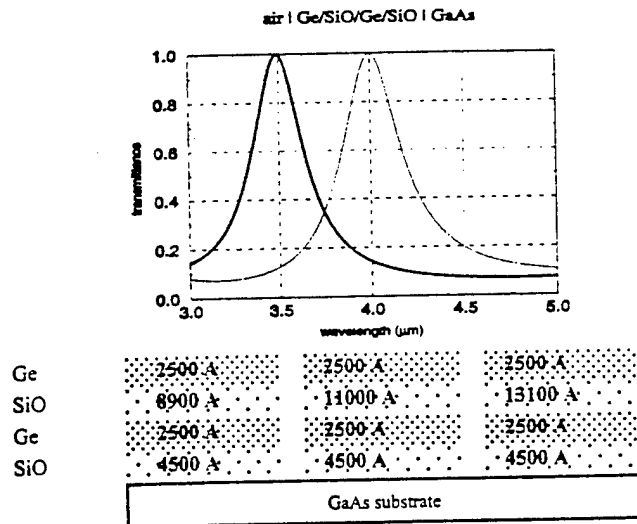


Figure 3. Calculated optimum structure of the multilayer subfilters on

materials, based on indices of refraction in the wavelength range of interest, compatibility with the substrates (sapphire and GaAs) and with themselves, and robustness to the atmosphere. Ge is widely available and is used as a high index material (refractive index  $n = 4.04$  at  $\lambda = 3.0 \mu\text{m}$ );<sup>17</sup> it is transparent in the 2-15  $\mu\text{m}$  wavelength range. SiO is often used as a low-index material up to a wavelength of 7  $\mu\text{m}$  for infrared multilayer filters. Its index of refraction is 1.80 at 4.0  $\mu\text{m}$ .<sup>18</sup> From a processing perspective, SiO is compatible with other oxides and metals such as Si, Ge, and Al. SiO is also used as protective overcoating for aluminum mirrors.

The substrates on which the sensors will be built are sapphire and GaAs. Sapphire is very hard and robust, and transparent in the wavelength range 0.14-6.5  $\mu\text{m}$ . GaAs has advantages over sapphire in terms of photolithographic etching and processing, and availability.

## 2. Computation of multispectral filter structures

Three sub-bandpass filters were designed with peaks at 3.5  $\mu\text{m}$ , 4.0  $\mu\text{m}$ , and 4.5  $\mu\text{m}$ , all within the 3-5  $\mu\text{m}$  range. Instead of attempting a narrow-band spectral characteristic with a large number of layers, the number of layers in each subfilter was minimized and priority was given to the structure that had the largest number of common layers for the three sub-filters, to assure a realizable and practical fabrication process. The optimum structure (minimum number of layers) for the interference subfilters was determined by a simulated annealing algorithm. Since the interference filters are not optimized outside the 3-5  $\mu\text{m}$  range, it will be necessary to cascade the interference subfilters with long-pass and short-pass absorption filters to reject light outside this

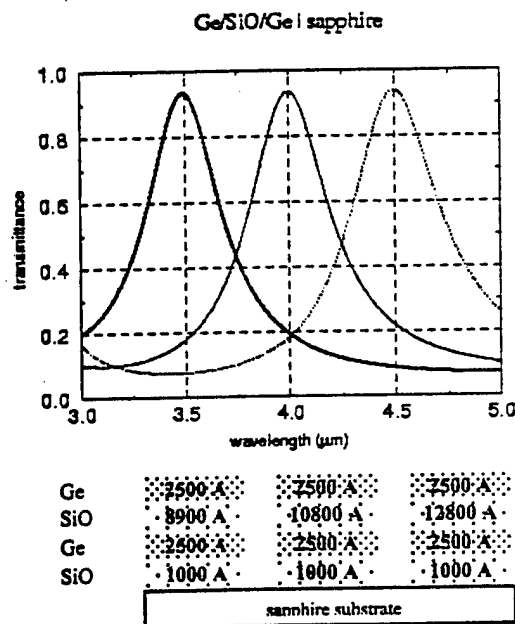


Figure 4. Optimum structure of the multispectral filters calculated for sapphire substrates

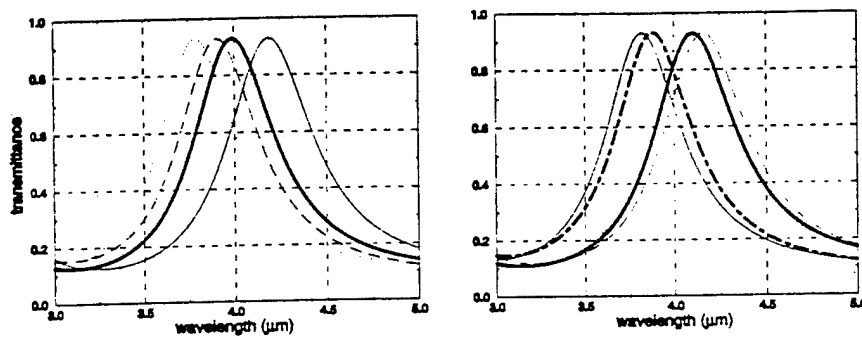
region. In the case of sapphire, the substrate itself can serve as the short-pass filter with its cutoff wavelength at about 6.5  $\mu\text{m}$ . The computation does not consider the effect of the backside reflection of the substrate, which decreases the transmitted light intensity by a constant factor.

Figures 3 and 4 show the simulated transmittance curves for the optimum structures on GaAs and sapphire substrates, respectively. Notice, from Figures 3 and 4, that in the case of sapphire substrates, the three-layer structure (without the first SiO layer) performs just as well as the four-layer structure. For GaAs, it was found that three layers never gave satisfactory results. It turns out that to achieve the desired three subfilters on a GaAs or sapphire substrate, the thickness of the middle SiO layer must be changed to shift the passband, as shown in Figures 3 and 4. This approach minimizes the number of sputtering and etching steps. In other words, for

the four-layer structure on a GaAs substrate, only two sputtering runs, rather than 12, are needed to deposit the three sub-filters.

Figure 5 shows the sensitivity of the filter transmission curve to potential fabrication errors in thicknesses of the various layers. This figure was generated for the four-layer structure on a sapphire substrate for the waveband that peaks at 4  $\mu\text{m}$ , assuming 5% of error in the film thickness. It can be concluded that the desired transmittance curve is shifted, while the shape of the curve is conserved by the variation of the film thickness.

air | Ge/SiO/Ge/SiO | sapphire



|     | dot | long-dash | solid2 | solid1 |     | solid2 | solid1 | dot | long-dash | dot-dash2 |
|-----|-----|-----------|--------|--------|-----|--------|--------|-----|-----------|-----------|
| Ge  | -5% | 5%        | 0      | 5%     | Ge  | 0      | 0      | -5% | 5%        | 5%        |
| SiO | -5% | -5%       | 0      | 5%     | SiO | 5%     | -5%    | 5%  | 5%        | -5%       |
|     |     |           |        |        | Ge  | -5%    | -5%    | -5% | 0         | 0         |
|     |     |           |        |        | SiO | 5%     | 5%     | 0   | -5%       | 5%        |

Figure 5. Calculated sensitivity of the multispectral filter to the thickness variation

### 3. Fabrication of the Multispectral Interference Filter

The triple-decker system was chosen for fabrication, because the double-decker system has many more difficult processing steps than the triple-decker design. Specifically, the difficulty stems from the large height differences between the multispectral subpixels ( $\sim 2 \mu\text{m}$  thick) and polarization subpixels ( $\sim 0.05 \mu\text{m}$  thick) which are contiguous in the case of the double-decker

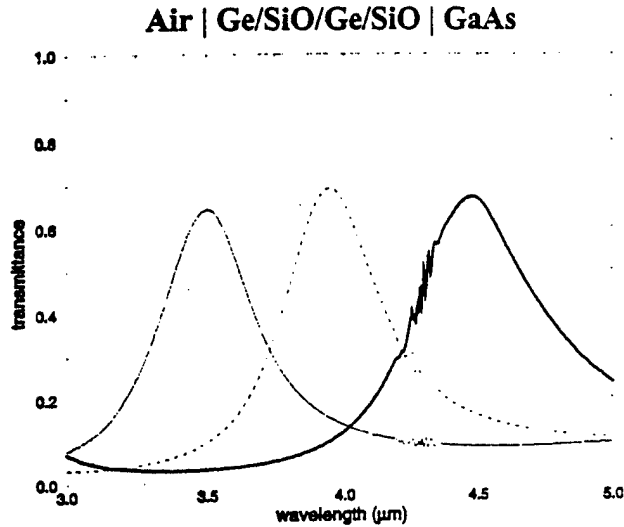


Figure 6. Transmission characteristic of multispectral filter on GaAs substrate

design.

The parameters used in the present sputtering experiments are 100 W applied to the plasma for Ge and 150 W for SiO with  $5 \times 10^{-3}$  torr of Ar under lower than  $1 \times 10^{-5}$  torr of base pressure. The deposition rates obtained with these parameters are 2.4 Å/sec for Ge and 1.7 Å/sec for SiO. It was also found that the refractive index of sputtered SiO is decreased by 10% due to the slow deposition, which confirms previous observations.<sup>19</sup>

The location of the peak is controlled by changing the thickness of the middle SiO layer in the film. To better control the peak location, the second SiO layer, where the multispectral filter will be patterned, was overgrown and then dry-etched afterwards under the parameters of 50 W and 10 sccm of  $\text{CF}_4$ . The subsequent patterning of the filters at shorter wavelength was done by follow-on dry-etching steps.

As a result, multispectral filters with three bands have been fabricated on GaAs and sapphire substrates. Figures 6 and 7 show the transmission characteristics of the multispectral filters on GaAs and sapphire substrates, respectively. In Figure 6, the spectral peaks of the multispectral filter on GaAs were measured at 3.50  $\mu\text{m}$ , 3.95  $\mu\text{m}$ , and 4.48  $\mu\text{m}$ . This filter consists of four interchanging layers of SiO and Ge. The middle SiO layer was dry-etched to tune the peak wavelength at the target. The peak value of the spectra is much lower than 100% because of the refraction at the backside of the substrate.

Figure 7 shows the spectral characteristic of the multispectral filter on sapphire, along with the simulated results. With only three layers, this filter is more convenient to process and has the efficiency enhanced with less backside reflection of sapphire. The peaks are located at 3.52  $\mu\text{m}$ , 3.99  $\mu\text{m}$ , and 4.44  $\mu\text{m}$  and the bandwidth of the filter is somewhat larger than simulated,

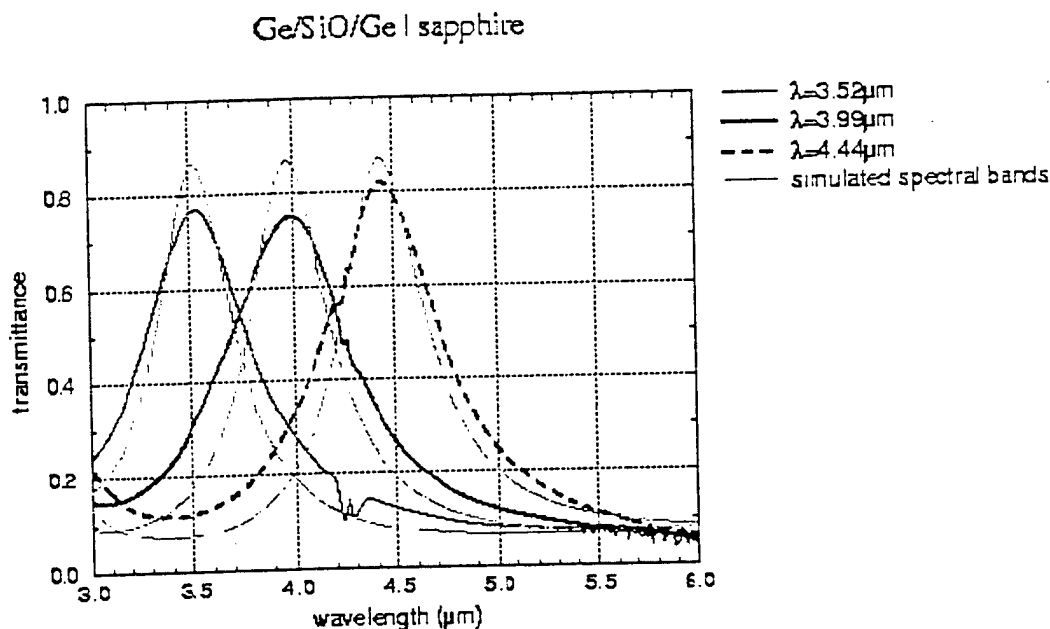


Figure 7. Transmission of the multispectral filter on sapphire

which is due to the non-uniformity of the middle SiO layer in the dry-etching process. Currently, the peak shift caused by the non-uniformity is less than 0.3  $\mu\text{m}$ . This non-uniformity is expected to be improved with several technical changes in the fabrication process. Each subpixel is formed in a stripe, 6 mm in width.

#### 4. Wire-grid polarization filter



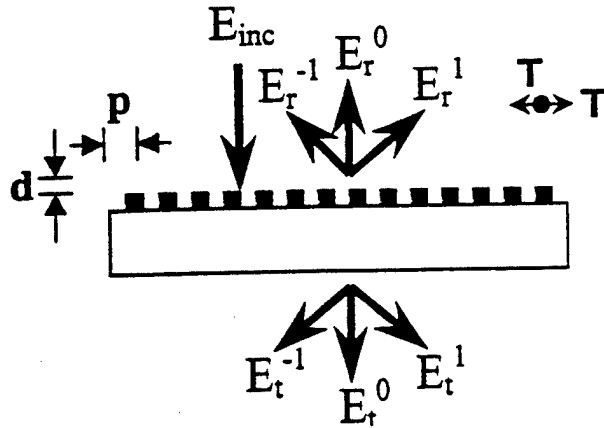


Figure 8. Schematics of the model in the wire-grid polarizer simulation

The structure of wire-grid polarizer was determined using GSOLVER 4.0, which is based on coupled-wave theory. In the simulation, it was assumed that the grating of the polarizer is of aluminum and the substrate is sapphire. Figure 8 schematically represents the model used in the computation. Note that the electric field of TM polarized light oscillates orthogonally to the gratings, while the TE component oscillates in parallel to the gratings.

Figures 9 and 10 show the transmittance dependence of TE or TM polarized incident light on the structural parameters such as grating height and grating period, respectively. For thick gratings, as in Figure 9, the TE polarization is much weaker with respect to the TM polarization and the extinction ratio, defined by  $|E_t^0_{TM}/E_t^0_{TE}|$ , becomes a large number. This means that the polarizer discriminates one polarization from the other very effectively for thick gratings. For the TM polarization, it is also interesting to observe the resonance dip. This resonance phenomenon, often called the 'Rayleigh anomaly', is due to the absorption of an incident plane wave and to the excitation of a surface wave to conserve momentum, with the repartitioning of the energy between several spectral orders.<sup>20</sup> In other words, the wire-grid polarizer will have higher-order diffracted light other than zero order, when the wavelength of the incident light is smaller than the wavelength of the Rayleigh anomaly. This occurrence of higher-order diffraction is evident in Figure 10, which shows the effect of different pitches on TE and TM polarizations for 0.75  $\mu\text{m}$  thick gratings. With a large pitch, the polarizer has a poor extinction ratio and the higher-order diffraction becomes a serious concern for MWIR wavelengths. This higher-order diffraction is undesirable, because this will degrade the signal-to-noise ratio of the sensor system.

This noise due to the higher-order diffraction, however, can likely be reduced or removed using several techniques. The most obvious is using very small pitch. According to Figure 10, the

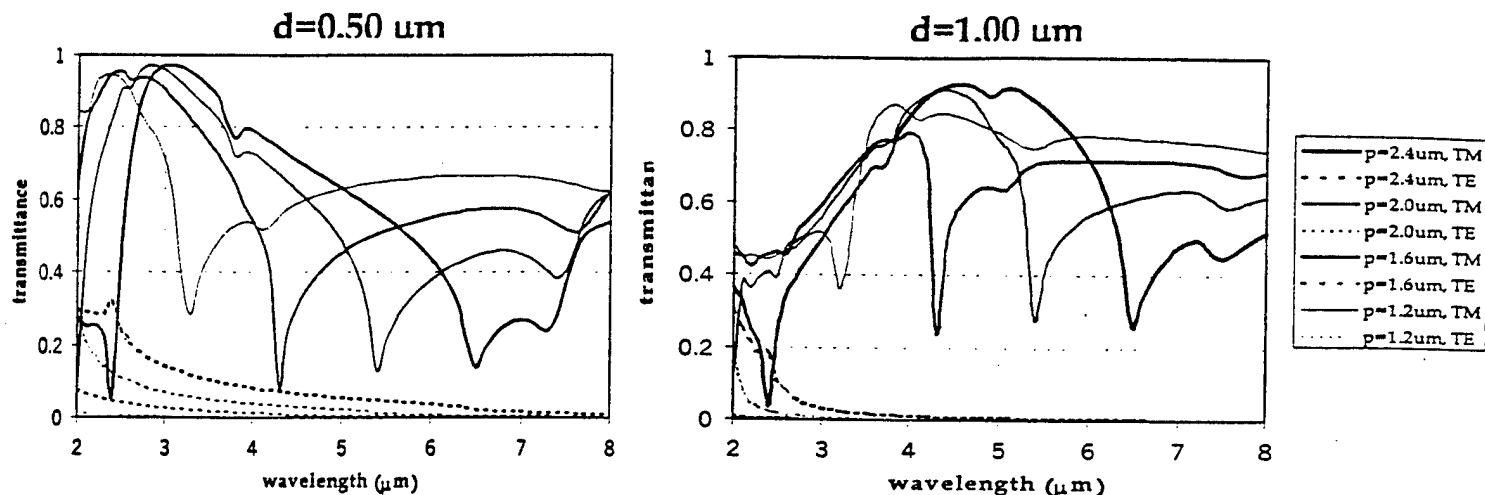


Figure 9. Effect of grating height (Al grating on sapphire substrate)

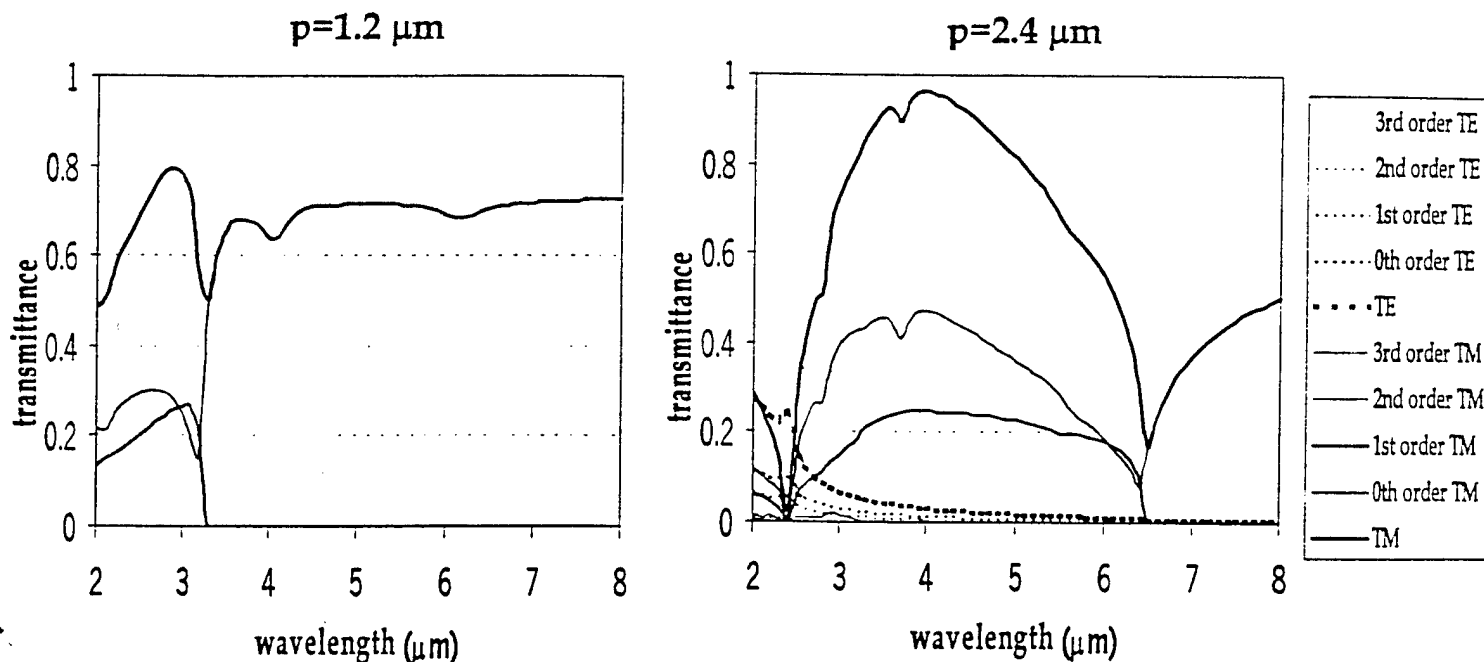


Figure 10. Effect of pitch at grating height =  $0.75 \mu\text{m}$  (Al grating on sapphire substrate)

polarizer with a grating pitch smaller than  $1.2 \mu\text{m}$  does not have higher-order diffraction for the 3-5  $\mu\text{m}$  wavelength range. It may also be possible to reduce the noise by adjusting the location of the wire-grid polarizer in the sensor system. For example, the noise can be removed by placing the polarizer far from the detector so that the diffracted light does not reach the detector.

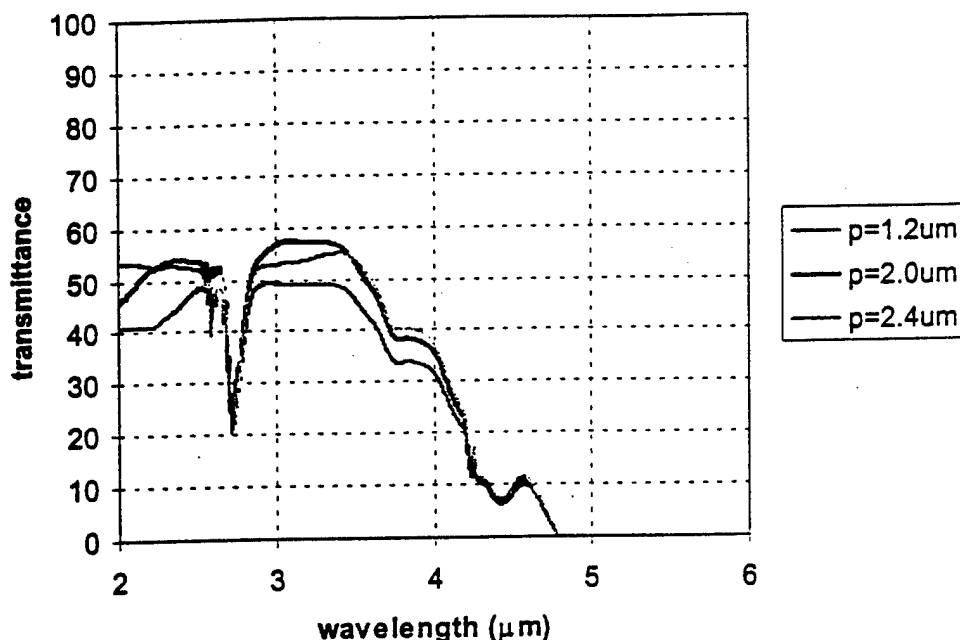


Figure 11. Transmittance of quartz mask for wire-grid polarizer

Based on the results of these simulations, the masks to fabricate the wire-grid polarizer were designed and ordered. In Figure 11, the transmittance of the received mask is shown, which was measured with FTIR spectroscopy.

## V. Future Direction and Concluding Remarks

In summary, using multiple sensors, which respond to different signature detection phenomena, increases the probability that a target can be identified against a given set of weather, clutter, or background noise sources. With an integrated sensor capable of discriminating between the spectral and polarization signatures of a target, improved image contrast can be achieved, because polarization and spatial signatures arise from the different optical characteristics of the target. Two structures were proposed for the sensor, and a triple-decker system is being developed because of processing simplicity. An optimum structure for the multispectral interference filter was determined based on a simulated annealing algorithm, and a multispectral filter plate has been fabricated on GaAs and sapphire. On the other hand, using coupled-wave

analysis, optimum structural parameters were estimated for a wire-grid polarizer. For reasonable processing difficulty with good extinction ratio, the optimal grating thickness is estimated to be between 0.5  $\mu\text{m}$  and 1.0  $\mu\text{m}$ . To remove high-order diffraction, the grating pitch needs to be smaller than 1.2  $\mu\text{m}$ .

The near-term processing efforts will be focused on the wire-grid polarizer fabrication based on optical lithography. Since the quartz mask of the polarizer itself is transparent for 3–4.5  $\mu\text{m}$ , the initial characterization effort will be made using the mask as a polarizer by mechanically contacting it with the fabricated multispectral filter.

When the fabrication of the wire-grid polarizer on sapphire substrate is complete, the characterization of the mechanically-contacted polarization filter with the multispectral filter and integrated multispectral polarization filter on the same substrate will be performed.

## References

- <sup>1</sup> R.D. Tooley, "Man-made target detection using infrared polarization," *Proc. of SPIE*, vol. 1166 Polarization Considerations for Optical Systems II, 33 (1989)
- <sup>2</sup> T.J. Rogne, F.G. Smith, and J.E. Rice, "Passive Target Detection using Polarized Components of Infrared Signature," *Proc. of SPIE*, vol. 1317 Polarimetry: Radar, Infrared, Visible, Ultraviolet, and X-Ray, 242 (1990)
- <sup>3</sup> T.J. Rogne, R. Maxwell, J. Nicoll, and R. Legault, "IR Polarization for Target Cuing," *Proc. IRIS Passive Sensors*, vol. 1, 323 (1997)
- <sup>4</sup> W.G. Egan, "Proposed design of an imaging spectropolarimeter/photopolarimeter for remote sensing of earth resources," *Opt. Eng.*, vol. 25(10), 1155 (1986)
- <sup>5</sup> W.G. Egan, "Polarization in remote sensing II," *Proc. of SPIE*, vol. 1166 Polarization Considerations for Optical Systems II, 23 (1989)
- <sup>6</sup> W.G. Egan, "Polarization in Remote Sensing," *Proc. of SPIE*, vol. 1747 Polarization and Remote Sensing, 2 (1992)
- <sup>7</sup> L.D. Travis, "Remote sensing of aerosols with the Earth Observing Scanning Polarimeter," *Proc. of SPIE*, vol. 1747 Polarization and Remote Sensing, 154 (1992)
- <sup>8</sup> P.Y. Deschamps, M. Herman, A. Podaire, and A. Ratier, "The POLDER Instrument: Mission Objectives," *Proc. of SPIE*, vol. 1747 Polarization and Remote Sensing, 72 (1992)

- <sup>9</sup> D.A. Glenar, J.J. Hillman, B. Saif, and J. Bergstrahl, "POLARIS II: an acousto-optic imaging spectropolarimeter for ground-based astronomy," *Proc. of SPIE*, vol. 1747 Polarization and Remote Sensing, 92 (1992)
- <sup>10</sup> D.H. Goldstein and R.A. Chipman, "Infrared spectropolarimeter," U.S. Patent #5,045,701 (1991)
- <sup>11</sup> D.B. Chenault and R.A. Chipman, "Infrared spectropolarimetry," *Proc. of SPIE*, vol. 1166 Polarization Considerations for Optical Systems II, 254 (1989)
- <sup>12</sup> B.H. Miles, E.R. Cespedes, and R.A. Goodson, "Polarization-Based Active/Passive Scanning System for Minefield Detection," *Proc. of SPIE*, vol. 1747 Polarization and Remote Sensing, 239 (1992)
- <sup>13</sup> C.S.L. Chun, D.L. Fleming, W.A. Harvey, E.J. Torok, and F.A. Sadjadi, "Synthetic vision using polarization-sensitive, thermal imaging," *Proc. of SPIE*, vol. 2736 Enhanced and Synthetic Vision, 9 (1996)
- <sup>14</sup> R.M.A. Azzam and K.A. Giardina, "Photopolarimeter based on planar grating diffraction," *J. Opt. Soc. Am. A*, vol. 10(6), 1190 (1993)
- <sup>15</sup> R.M.A. Azzam, "Diffraction-grating photopolarimeter and spectrophotopolarimeter," U.S. Patent #5,337,146 (1994)
- <sup>16</sup> J.R. Maxwell and T.J. Rogne, "Advances in Polarized Infrared Imaging, Part 1 & 2," *Spectral Reflections*, IRIA Newsletter, 97-01 & 97-04 (1997)
- <sup>17</sup> E.D. Palik, ed., *Handbook of Optical Constants of Solids* (Academic, New York, 1985), p.475
- <sup>18</sup> *Ibid.*, p. 768
- <sup>19</sup> W.A. Pliskin and H.S. Lehman, "Structural Evaluation of Silicon Oxide Films," *J. of Electrochem. Soc.*, vol. 112 (10), 1013 (1965)
- <sup>20</sup> For example, "*Electromagnetic Theory of Gratings*," ed. R. Petit, Springer-Verlag (1980)